A Geometrical Heuristic Image Processing Approach For The Automatic Detection & Quantification of Type-IV Crater Lesion Pathology In The Femoral Cartilage of The Human Knee

Zarrar Javaid *zarrar_j@yahoo.com*
Department of Engineering Science
The University of Auckland
Auckland, 1010, New Zealand

Fergus J. Perks *fperks@nhs.net*
Department of Clinical Radiology
Royal Infirmary of Edinburgh
Edinburgh, EH16 4SA, United Kingdom

Peter McNair *peter.mcnair@aut.ac.nz*
Health and Rehabilitation Research Center
Auckland University of Technology
Auckland, 0627, New Zealand

Charles P. Unsworth *c.unsworth@auckland.ac.nz*
Department of Engineering Science
The University of Auckland
Auckland, 1010, New Zealand

Abstract

The type-IV crater is a chondral lesion found in 5-10 percent of injured knees undergoing arthroscopy. The lesion is identified as a serious injury, being found predominantly in young adults, around 30 years of age, having the potential to quickly progress to osteoarthritis due to high load sporting activities typically pursued by this age group. In addition, pain and swelling often accompany larger lesions of this type, and it is recommended that treatment occurs as soon as possible while the lesion is well demarcated.

The main limitation, in the quantification of type-IV crater volumes in 'real' human knees is that it is not possible to obtain the true volumes of the craters through a physical experimental measure and manual delineation is known to suffer from user error.

We resolve this issue by performing extensive simulations of synthetic craters, of known radii and volume, within the femoral cartilage of 21 healthy knee joints to validate how a novel geometrical heuristic image processing approach can be used to detect type-IV crater lesions and quantify their volumes accurately in real-time from pre-segmented MR images which we compare to the standard manual delineation approach. We show that the mean %error in accuracy of our approach compared to the manual delineation approach for detecting and quantifying synthetic craters of 2-4 mm radii was significantly less ($P<0.05$) for our developed approach and the time was near instantaneous versus longer times required for manual delineation.

Finally, we demonstrate how our developed approach could be used to detect type-IV crater pathology in a randomized sequence of 21 healthy and 4 real pathological knees (containing 5 type-IV craters in total). We show how our developed approach could identify real pathological from non-pathological knees with 100% accuracy ($P<0.001$). In addition, it was found that our developed approach could identify anatomical location of the real type-IV craters to be the same as a blinded operator's identification of the position of craters (Kappa=1). Furthermore, since our developed approach performed better than the standard manual delineation approach from the

synthetic crater results, we applied it as the benchmark for the quantification of real type-IV crater volumes, and demonstrate how the manual delineation approach underestimated the real type IV crater volumes with a mean %error of 1.7% which was found to be consistent with the synthetic simulations.

In conclusion, we demonstrate how a novel geometrical heuristic image processing approach can provide accurate real-time, automatic detection and quantification of type-IV crater lesions in pre-segmented MR images of the femoral cartilage for radii 2-5 mm. To the authors knowledge this is the first time type-IV crater lesions in the MR image of a human femoral cartilage have been detected and quantified automatically.

Keywords: Type-IV Crater Lesions, Femoral Cartilage, MR Images, Pathology, Automatic Detection.

1. INTRODUCTION

Chondral Injury (CI) in the articular cartilage can lead to Osteoarthritis (OA) [1], a global cause for disability in people over 65 years. Quantifying lesions in cartilage early and accurately may allow more effective assessment and implementation of treatment regimes to slow the overall progression of the disease. CI manifests itself in six lesion subtypes as classified in Bauer et al 1988 [2]: type-I, linear crack; type-II, stellate fracture; type-III, flap; type-IV, crater; type-V, fibrillated; and type-VI, degrading. Arthroscopy has traditionally been seen as the gold standard for detecting articular cartilage lesions, having accuracy of 95-98% [3-5]. However, arthroscopy is invasive and expensive and has inherent potential complications for patients compared to conservative assessments [6, 7]. An alternative to arthroscopy is Magnetic Resonance Imaging (MRI). Using this technology, measures of volume and thickness of the articular cartilage [8] are used for identifying chondral lesions [9-13]. MR images of the knee articular cartilage are often classified by the Outerbridge grading system [2, 14-17].

The type-IV crater is a rare chondral lesion found in 5-10 percent of injured knees undergoing arthroscopy (12% in 31,516 knees [18] and 6.6% [19] in 1,260 knees), and is most commonly located on the medial femoral condyle [20]. It is associated with other soft tissue pathology such as ACL rupture [21] and meniscal tears [22]. The lesion is regarded as serious, and as it is often found in younger patients (30 years old) [20], the potential for progression to osteoarthritis is greater, particularly if the patient continues to engage in high load activities such as jumps and landings. Pain and swelling are often apparent in larger lesions of this type, and it is recommended that treatment occurs as soon as possible while the lesion is well demarcated [23].

To date, automatic detection and quantification techniques for lesions such as type-IV craters have not been developed [2] and manual methods can become laborious and time consuming, with greater potential for errors being made by an operator digitizing scans. Hence, our motivation is to provide a heuristic approach for early diagnosis and accurate quantification of this type of lesion with this work. Thus, this article presents a geometrical heuristic image processing approach that can automatically detect and quantify type-IV lesions accurately in real-time. With further development, this may eventually serve as a point-of-care, 3D visualization tool to assist a consultant radiologist in diagnosis of such pathologies. To our knowledge this is the first time type-IV crater lesions in the MR image of a human femoral cartilage have been detected and quantified automatically.

2. MATERIALS AND METHODS

2.1 Data and Resources Used

All subjects provided written informed consent and institutional ethics approval was granted for this study. MR scans of 25 knees from 9 Males (ages 27-55) and 12 females (ages 30-61) subjects (M1–M25) were used. 21 healthy knees were obtained using a Philips Medical Systems 1.5-T Gyroscan-Intera whole-body scanner with an extremity quadrature coil (Medical Advances

Inc.). Healthy knees were imaged in the sagittal plane with T1-weighted fat-suppressed 3D spoiled gradient recalled acquisition in steady state. An image sequence, size 512x512, slice thickness 1.5mm, field of view 160mm; flip angle 55^{o}; repetition 57ms, echo time 12ms respectively. At a later data collection point, a Siemens Magnetom-Skyra-syngo MRD was utilized, and four knees with pathology were imaged and examined by a clinical expert, and subsequently compared to 21 healthy knees utilizing the automated and manual delineation techniques.

In this paper, we apply our developed geometrical heuristic approach to manually pre-segmented MR images. We initially define a minimum search criteria for type-IV craters [2], describe the methodology developed to detect and quantify type-IV crater lesions and perform three investigations to validate performance of the method (referred to as the '**Automated method'**) and compared this to standard manual delineation (referred to as the '**Manual method**'). Finally, we provide a comparison of the volumes of 'real' type-IV craters estimated from the automated and manual methods.

2.2 Methodology

We perform 2 studies to demonstrate our developed automated method.

2.2.1 Study 1: Synthetic Crater Assessment of Manual & Automated Methods

The main limitation, in the quantification of type-IV crater volumes in 'real' human knees is that it is not possible to obtain the true volumes of the craters through a physical experimental measure and manual delineation is well known to suffer from user error [24]. In this study, we resolve this issue by performing extensive computer simulations of synthetic craters in manually segmented MR images of the femoral cartilage of healthy knees. This was performed by generating synthetic craters of known volumes (i.e. by setting pixels to a grayscale of 0), and inserting these into several MR slices of each of the 21 healthy knees. It should be noted that the actual cartilage that was deleted was solid and filled the region of deletion uniformly. We defined a reasonable minimum depth of a type-IV crater lesion to be at least two consecutive slices of articular cartilage, which corresponded to a depth ≥ 1.5 mm. Hence, we generated 80 synthetic craters of radii 2-5mm (Figure 1) in the medial condyle, lateral and medial trochlea, lateral tibial-femoral interface and lateral condyles of the MR slices of the 21 healthy knees because real type-IV crater occurs primarily in these regions.

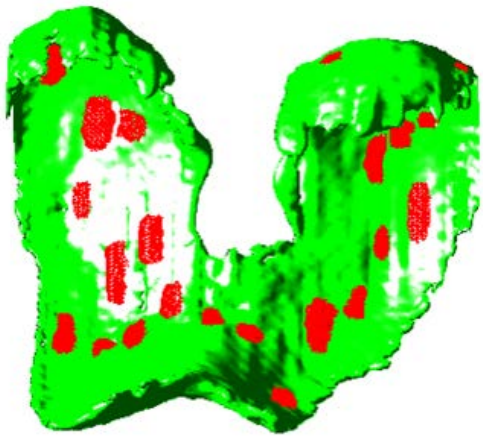

FIGURE 1: A 3D view of the femoral cartilage with typical synthesized craters of radii 2-5mm.

We then proceeded to assess the accuracy of the manual and developed automatic methods against the known crater volume. Crater delineation was performed once daily and repeated over 3 days (resulting in 240 synthetic holes being measured) for both manual and automated

methods. A paired t-test [25] was utilized to assess the difference in the mean %error in volume across the manual and automated methods (α=0.05).

2.2.2 Study 2: Detecting Knees with Pathology & Type-IV Crater Quantification

In Study 2, the manual and automated methods were used to identify which knees exhibited type-IV crater pathology from a randomized series of 21 normal knees and 4 with pathology (containing five type-IV craters in total). (Figure 2,a-d) presents all the real type-IV craters (shown in red) in their respective femoral cartilage 3D model, reconstructed with Javaid et al. [26]. A blinded operator was used to identify the anatomical locations of the real type-IV craters.

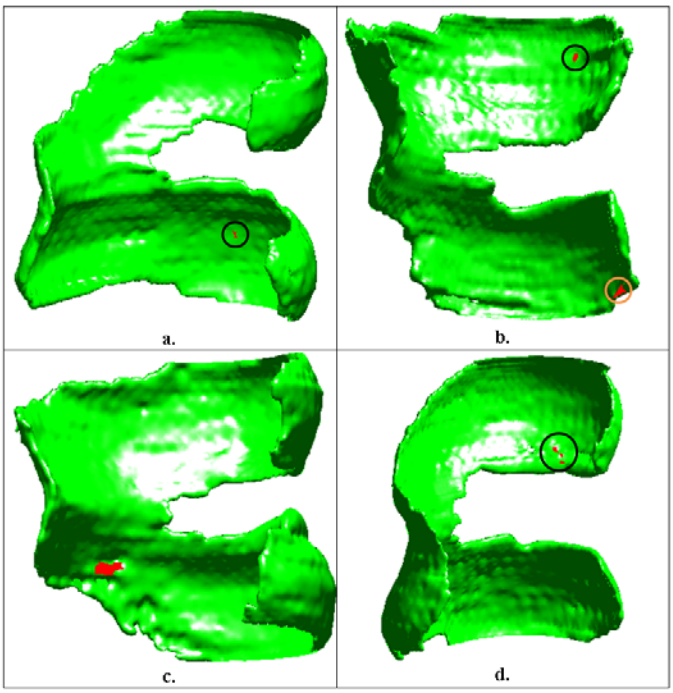

FIGURE 2: 3D model of the femoral cartilage of: (a) M1 left knee with type-IV crater 1 at the lateral tibial-femoral interface encircled in black. (b) M3 right knee with type-IV crater 2 on the medial condyle encircled in orange and type-IV crater 4 on the lateral condyle encircled in black. (c) M1 right knee with type-IV crater 3 (red) on the medial trochlea. (d) M3 left knee with type-IV crater 5 on the medial condyle encircled in black.

The locations of the five type-IV craters in the 4 pathological knees were then compared between an independent operator (blinded to the pathology of the scans) and the developed automated method to assess how well the locations of the injury correlated in slice number and anatomical location and volume. A paired t-test was used to compare the number of slices that the type-IV craters were identified to occur in from both manual and automated methods (α=0.01). A Kappa statistic was used to measure the operator's agreement in location of the type-IV craters to the automated method. Since we demonstrated, in Study 1, how the developed automated method was significantly more accurate for synthetic holes than conventional manual delineation, we elected to measure the mean %error of the estimated volume of the manual method relative to the automated method, hence, highlighting how our technique works for real cases.

2.2.3 The Developed Geometrical Heuristic Method for Type-IV Crater Detection

The development of our automated method involved three phases. Firstly, identification of true type-IV crater faces, thereafter identifying the end points of the true type-IV crater lesion faces and finally delineating the type-IV crater and estimating the crater volume. These phases are described below. We defined a reasonable minimum criterion for a type-IV crater lesion to exist in at least two consecutive slices of articular cartilage, which corresponds to type-IV crater lesions of depth ≥ 1.5 mm.

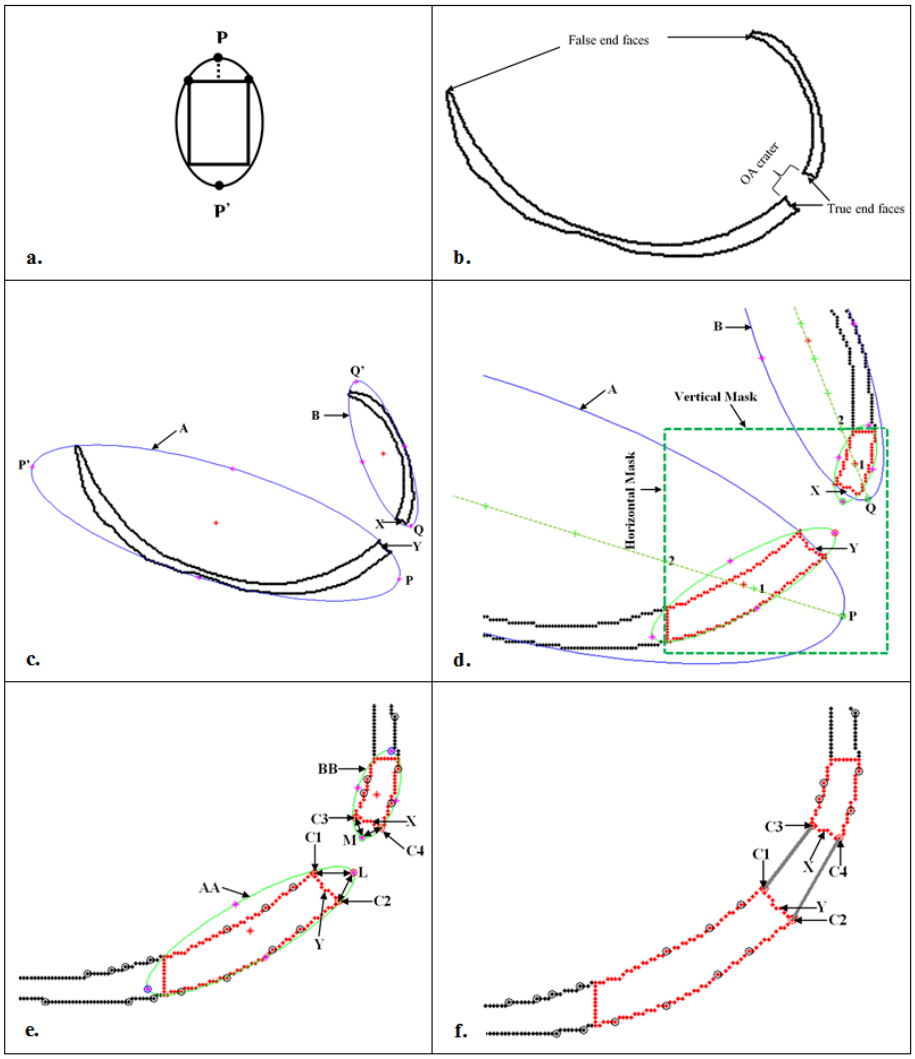

FIGURE 3: (a) MVEE enclosing a linear object (b) True and false end faces of the contours forming a type-IV crater (c) Initial MVEE (blue) fitted around the cartilage contours (d) New ellipses (light green) fitted to the linearized cartilage portion (red dots). Light green '+' highlights linear interpolated major axes. The dark green box represents the mask used to segment the two pieces of cartilage (e) Probable corners (black circles) identified by Harris method on the cartilage contours. (f) True corner points C1-C4 of a type-IV crater (small red circles) with delineated crater (grey lines) identified by our automated method.

A. Identify the True Type-IV Crater Faces

Initially, to identify a type-IV crater face we apply a novel adaptation of Moshtagh's method [22]. Moshtagh's method [22] was originally developed to determine the area of a linear object by enclosing it in a minimum volume enclosed ellipsoid (MVEE) (Figure 3a). However, we do not use Moshtagh's method to find the area of an object but rather adapt the MVEE part of the work to locate the true faces of a type-IV crater.

We define two sets of contour faces: 'true end faces' being the desired faces of the contour that we wish to identify and 'false end faces' being the other end faces of the contours, (Figure 3b). We then fit an initial MVEE to each contour of the cartilage, (Figure 3c). The distances from the end points (P, P') of the major axes of ellipse A to all the end points (Q, Q') of the major axes of ellipse B were computed and the end points of the major axes of the two ellipses which are at a minimum distance apart (P, Q) locate the approximate location of the true end faces of the contour (faces 'X' and 'Y', Figure 3c).

Unlike Moshtagh's MVEE method, the major axis end points (P, P' and Q, Q') of the ellipsoids do not center at the faces due to the non-linear nature of the contours. However, we identified that this can be resolved by, refining the ellipse position. This can be achieved by linearly dividing the major axes of ellipse A and B into a series of 10 uniformly spaced divisions, Figure 3d (green '+'). We determined that a vertical mask subtended from the 2nd division from P and a horizontal mask subtended from the 2nd division from Q (dark green box, Figure 3d) provided 2 smaller contours (Figure 3d, red dots) which were approximately linear. We then reapplied MVEE to these regions to obtain new ellipses (AA and BB, Figure 3e).

B. Automatically Identifying the End Points of the True Type-IV Crater Lesion Faces

To identify the end points of the type-IV crater lesion faces, we employed Harris's corner detection method [27] and Moshtagh's (MVEE) method for a third time. Hence, all probable corner points (black circles) on the cartilage were identified, (Figure 3e).

To identify the true corners from the probable corners, we found that the two minimal distances between the major axis point L of ellipse AA and all the probable corner points determined on the cartilage contour enclosed by ellipsoid AA identified the true corners (C1 and C2, Figure 3e) at face 'Y'. Similarly, the true corners (C3 and C4, Figure 3e) could be identified on ellipse BB at face 'X'.

C. Delineate the Type-IV Crater and Estimate Crater Volume

Next, points C1-C4 were connected using a shortest distance approach between the opposite corner points (grey lines, Figure 3f). The volume of the delineated type-IV crater was estimated using Cheong's method [28] which employs Caverlieri's principle [29] where the sum of the crater area is multiplied by the inter-slice distance.

3. RESULTS

3.1 Study 1: Synthetic Crater Assessment of Manual & Automated Methods

It was found that the time required for an operator to look through the 60 MR image slices manually of a knee and delineate a type-IV crater manually was 10 minutes. Since this was performed on 3 separate days to reduce user error in the delineation of the crater, a conservative estimate of the total time required to find and delineate a crater manually over the 3 days was 30 minutes. The time required for the developed automated method to process the 60 MR image slices of a knee, delineate a type-IV crater and calculate the volume of the crater was found to be near instantaneous on all days, leading to a real-time detection and quantification of type-IV craters for the automated method. The variable of interest was the mean %error in volume from the known true volume of the synthesized type-IV craters, and this was calculated for both the manual and automated methods.

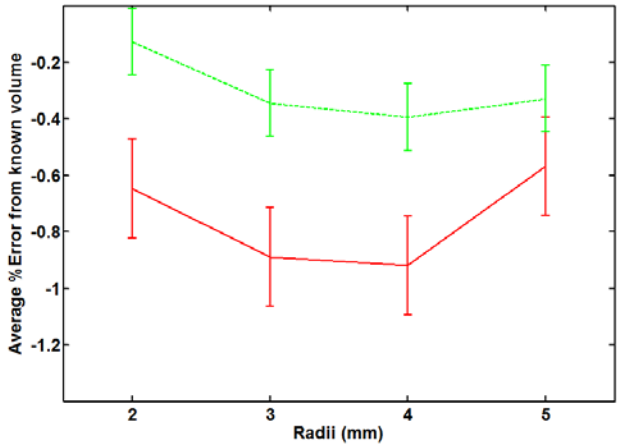

FIGURE 4: The mean %error from known synthesized crater volumes vs. crater radii of the synthesized type-IV craters for manual method (red solid lines) and automated method (dotted green lines).

It was found that the mean %error (Figure 4) for the automated method from the known volumes of craters of 2-4mm radii was statistically significant over the manual method, providing p-values of 0.0464, 0.0083 and 0.0428 respectively. It was found that whilst the automated still improved upon the manual method for 5 mm crater radii, there was no significant difference (p= 0.3087) between the techniques. In addition, the time to detect and quantify a crater manually was of the order of a several minutes compared to the automated technique which is nearly instantaneous for all type-IV crater lesions of 2-5mm.

3.2 Study 2: Detecting Knees with Pathology & Type-IV Crater Quantification

Crater Number	Operator location	**Automated Method location**	**No. of Slices in Crater identified by**	
			Operator	**Automated Method**
Crater 1	M1 (left) / Lat Tib-Fem	M1 (left) / Lat Tib-Fem	2	2
Crater 2	M3 (right) / Med Condyle	M3 (right) / Med Condyle	2	2
Crater 3	M1 (right) / Med Trochlea	M1 (right) / Med Trochlea	3	3
Crater 4	M3 (right) / Lat Condyle	M3 (right) / Lat Condyle	2	2
Crater 5	M3 (left) / Med Condyle	M3 (left) / Med Condyle	3	3

TABLE 1: Summary of Real Type-IV Crater lesion identified manually and automatically. *Note all 21 healthy knees (not shown here) had the number of slices set to a zero by an independent operator when found not to have pathology.

For the 21 healthy knees, it was found that no craters were detected by the blinded operator or our developed automated method and in the pathological knees all locations of the lesions (N=5) were identified (see Table 1) by both. For knees with pathology, where a type-IV crater was found, the total number of MR slices that the type-IV crater spanned was noted (in column 4, Table 1). In the case of a healthy knee, where no crater was found, the number of slices (in column 4, Table 1) was set to 0 by the blinded operator (not shown in Table 1 for conciseness). Similarly, the number of slices (in column 5, Table 1) was set to 0 by the automated method (not shown in Table 1 for conciseness) when no crater was present. Thus, using a paired t-test on all the slices values of the 4 knees with pathology and the 21 healthy knees, it was possible to determine that the automated method identified which knees had pathology or not to 100% accuracy and additionally identifies the number of slices that a crater had to 100% accuracy (p-value <0.001). Thus, both the anatomical locations of the real type-IV craters and the number of MR slices that they existed in were found to be the same as identified by a blinded operator and the automated method.

For the five type-IV crater lesions identified in (Figure 2) by the blinded operator, we compared the volumes quantified by the standard manual delineation method to our developed automated method. The estimated volumes of the real type-IV craters are summarised in Table 2. And each crater detected is subsequently described.

Subject (knee position)/Location	Estimated Volume in mm^3		Mean %Error
	Mean Automated ± SD	Mean Manual ± SD	Manual (w.r.t mean Automated)
M1 (left) / Lateral Tibial-Femoral	6.12 ± 0	6.01 ± 0.077	-1.71
M3 (right) / Medial Condyle	21.4 ± 0	21.11 ± 0.519	-1.32
M1 (right) / Medial Trochlea	84.56 ± 0	83.37 ± 0.969	-1.41
M3 (right) / Lateral Condyle	6.05 ± 0	5.91 ± 0.109	-2.39
M3 (left) / Medial Condyle	17.02 ± 0	16.73 ± 0.062	-1.68

TABLE 2: Summary of the Estimated Volume and Mean %Error of the Real Type-IV crater.

A. Real Type-IV Crater 1

Type-IV crater 1 was located on the left knee lateral tibial-femoral interface of subject M1. It had 2 slices where the crater was approximately the same area at each slice (Figure 5a-c). It was found that the mean %error of the estimated volume of the manual method with respect to the automated method was -1.71% (that is the manual method underestimated the crater volume), Table 2.

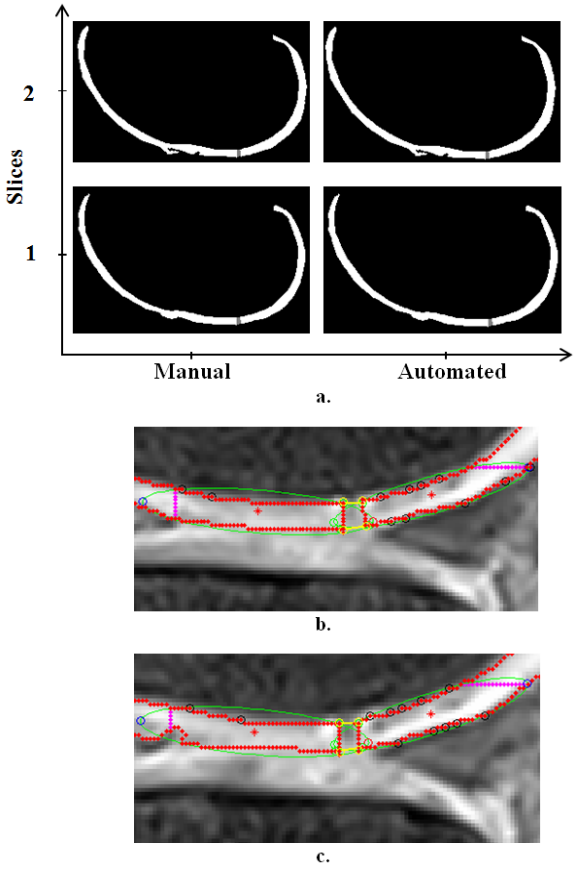

FIGURE 5: (a) Femoral cartilage slices of M1 left knee with a 2-slice hole at the lateral tibial and femoral cartilage interface filled using manual and automated methods. M1 left knee lateral tibial-femoral cartilage interface (b) slice1 and (c) slice 2: Manually delineated (red) cartilage with manually identified crater corners (yellow circles) and automatically detected crater corners (green circles). Yellow lines highlight the automated delineation of the type-IV crater using our automated method.

For visualisation purposes, we highlight the 3D rendering of type-IV crater 1 (Figure 6a-b) using the reconstruction method of Javaid et al. [26]. It can be seen that the 3D volume is uniform through both slices as expected from our observations of Figure 4a.

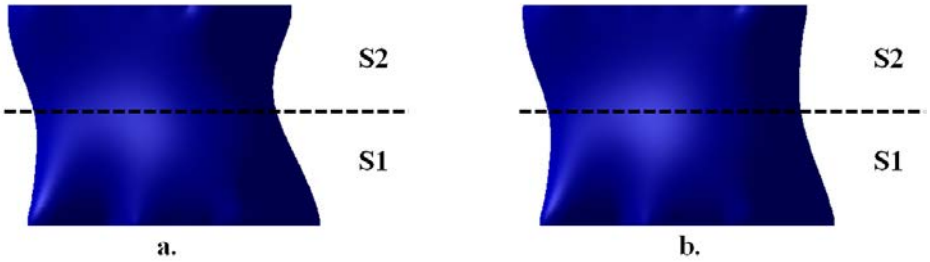

FIGURE 6: M1 left knee 2-slice (S1-S2) type-IV crater at the lateral tibial femoral interface (a) 3D model of the manually delineated type-IV crater 1 (b) 3D model of the automatically delineated type-IV crater 1.

The volume of the type-IV crater was estimated using Caverlieri's principle [29] used by Cheong [28]. Estimated volumes of the type-IV crater were calculated for both manual and automated methods. As the statistical analysis of the synthetic craters demonstrated that our automated method was more accurate than the manual method (determined from the synthetic experiments) we used the volumes calculated from the automated method as the new benchmark from which the mean %error was referenced to. A summary of the estimated volumes of the real type-IV craters for the two methods is given in Table 2. The mean %error of the manual with respect to the mean estimated volume of the automated method is also presented in Table 2.

B. Real Type-IV Crater 2

Type-IV crater 2 was located on the medial condyle of the right knee of subject M3 with 2 slices. It is observed (Figure 7a-c) that the crater size decreases as we move from slice 1 to 2. It was found that the mean %error of the estimated volume of the manual method with respect to the automated method was -1.32% (that is manual under estimate the crater volume), Table 2.

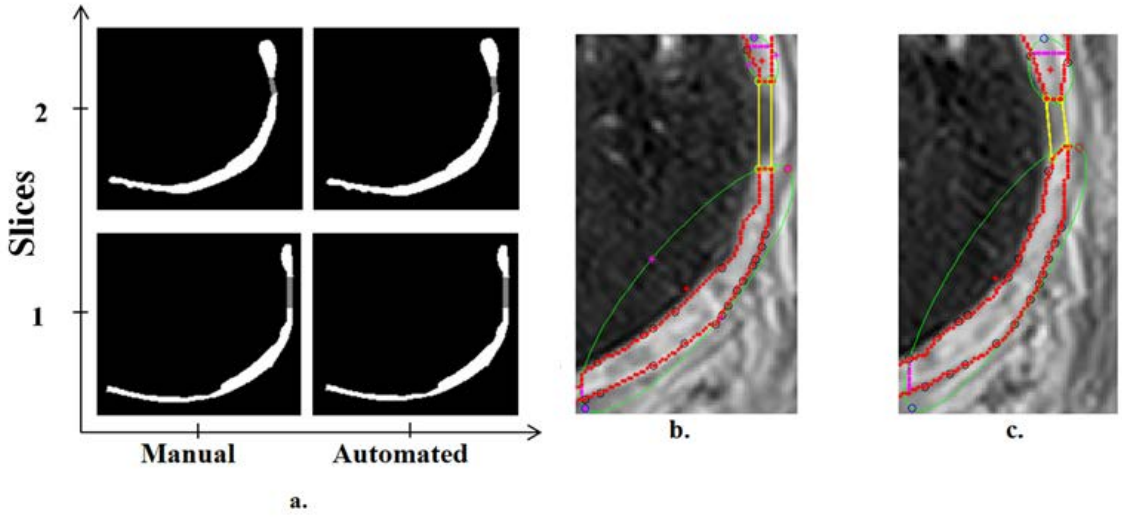

FIGURE 7: Type-IV crater 2 (a) Femoral cartilage slices of M3 right knee with a 2-slice crater in the medial condyle filled using manual and automated methods. MRI of (b) slice 1 and (c) slice 2 of crater 2: Manually delineated (red) cartilage with manually identified crater corners (yellow circles) and automatically detected crater corners (green circles). Yellow lines highlight the automated delineation of the type-IV crater lesion using our automated method.

C. Real Type-IV Crater 3

Type-IV crater 3 was located on the right knee medial trochlea of subject M1 with 3 slices. It is observed (Figure 8a-d) that the crater size decreases as we move from slice 1 to 3. It was found that the mean %error of the estimated volume of the manual method with respect to the automated method was -1.41% (that is manual under estimate the crater volume), Table2.

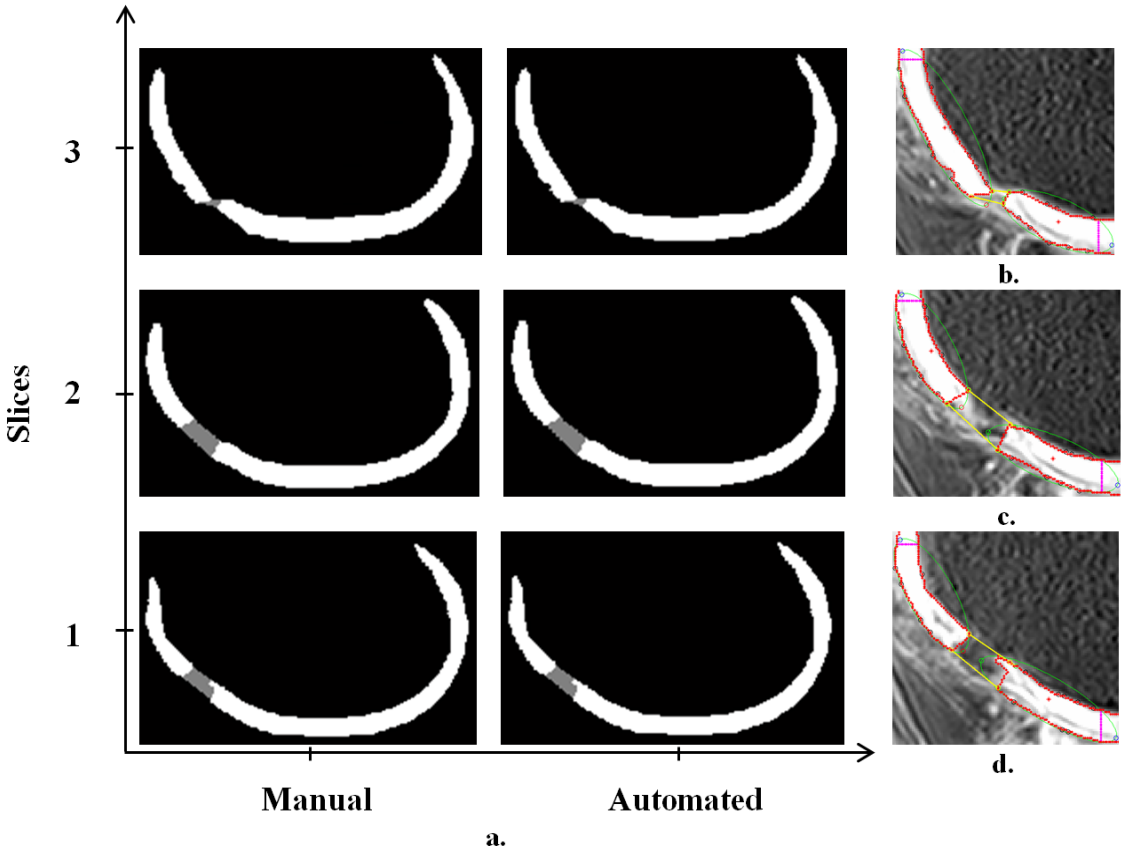

FIGURE 8: Type-IV crater 3 (a) Femoral cartilage slices of M1 right knee with a 3-slice crater in the medial trochlea filled using manual and automated methods. MR images of (b) slice 3 (c) slice 2 and (d) slice 1 of crater 3: Manually delineated (red) cartilage with manually identified crater corners (yellow circles) and automatically detected crater corners (green circles). Yellow lines highlight the automated delineation of the type-IV crater lesion using our automated method.

D. Real Type-IV crater 4

Type-IV crater 4 was located on the lateral condyle of the right knee of subject M3 with 2 slices. It is observed (Figure 9a-c) that the crater size decreases as we move from slice 1 to 2. It was found that the mean %error of the estimated volume of the manual method with respect to the automated method was -2.39% (that is manual under estimate the crater volume), Table 2.

E. Real Type-IV crater 5

Type-IV crater 5 was located on the left knee medial condyle of subject M3 with 3 slices. It is observed from (Figure 10a-d) that the crater is roughly of the same size but staggered to the left as one moves from slice 1 to 3. It was found that the mean %error of the estimated volume of the manual method with respect to the automated method was -1.68% (that is manual under estimate the crater volume), Table 2.

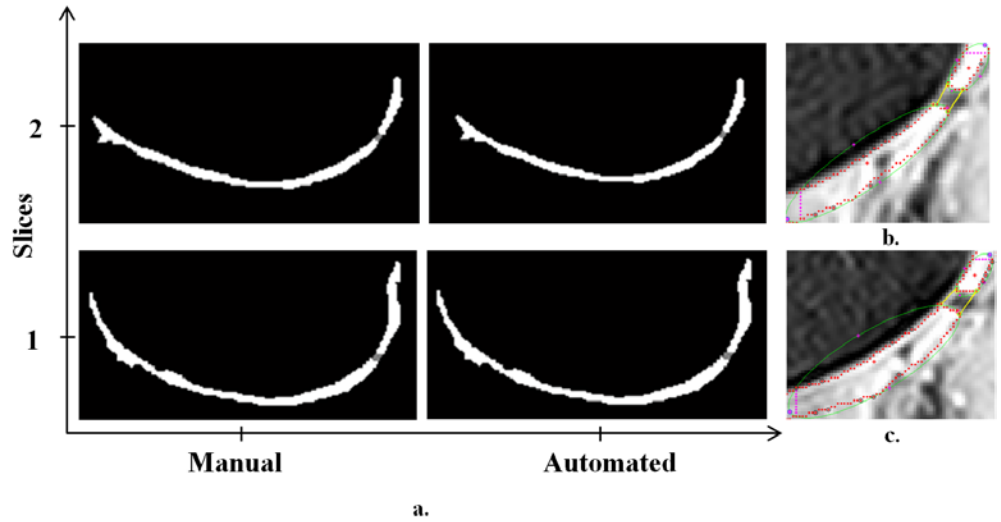

FIGURE 9: (a) Femoral cartilage slices of M3 right knee with a 2-slice crater in the lateral condyle filled using manual and automated methods. M3 Right knee lateral condyle (b) slice 2 and (c) slice 1: Manually delineated (red) cartilage with manually identified crater corners (yellow circles) and automatically detected crater corners (green circles). Yellow lines highlight the automated delineation of the Type-IV crater lesion using our automated method.

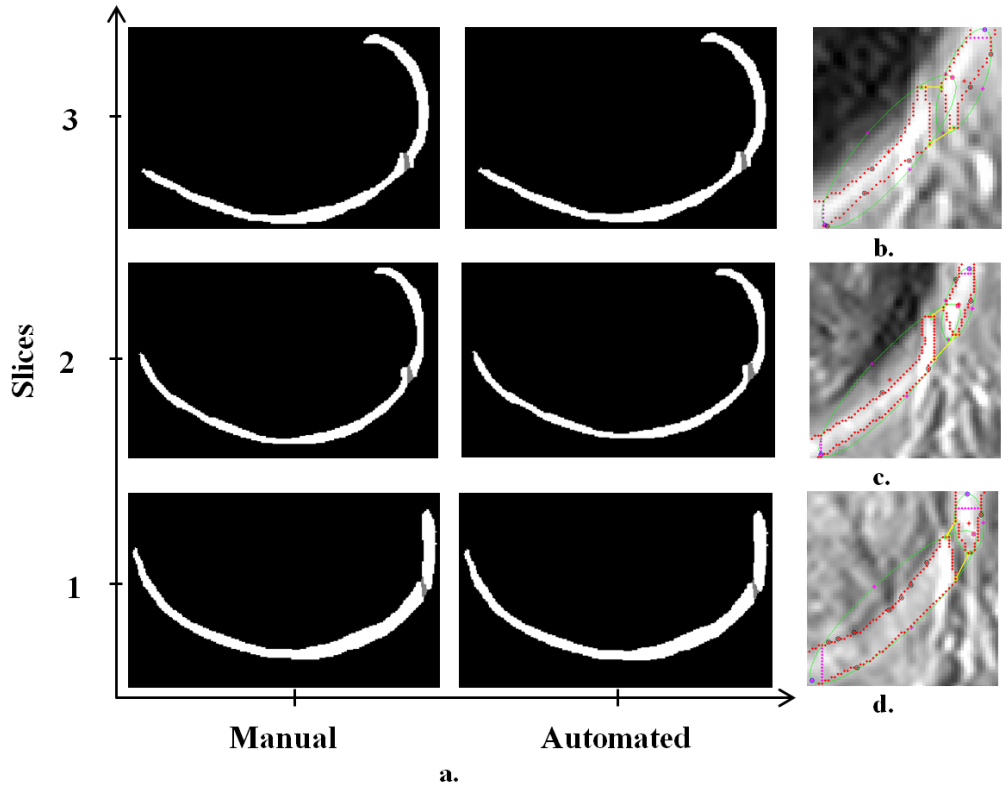

FIGURE 10: (a) Femoral cartilage slices of M3 left knee with a 3-slice crater in the medial condyle filled using manual and automated methods. The fill is shown in grey colour. M3 left knee medial condyle (b) slice 3 (c) slice 2 and (d) slice 1: Manually delineated (red) cartilage with manually identified crater corners (yellow circles) and automatically detected crater corners (green circles). Yellow lines highlight the automated delineation of the Type-IV crater lesion using our automated method.

One observes from Table 2, that the mean estimated volume of all the craters of the automated method is greater than the mean estimated volume of the manual method. Thus, now using the automated method as the new benchmark it can be concluded that the manual method underestimated the crater volume. This under-estimation was found to be consistent with the synthetic results, Figure 4, where the manual method always underestimates in comparison to the developed automated method for known volumes.

4. CONCLUSION

This article presents a novel geometrical heuristic image processing approach that can accurately, automatically detect and quantify type-IV crater lesions in real-time. To our knowledge this is the first time type-IV crater lesions in the MR image of a human femoral cartilage have been detected and quantified automatically.

Since it is not possible to quantify type-IV crater volumes in 'real' human knees through a physical experimental measure, we pragmatically performed extensive simulations in the creation of 80 synthetic craters, of known radii and volume, within the MR images of 21 healthy knee joints. This allowed us to explicitly determine how well the developed method worked and compare it to standard manual delineation. Results demonstrated that the mean %error of the automated method for craters of 2, 3 and 4 mm radii was statistically significant in accuracy over the manual delineation method giving p-values of 0.0464, 0.0083 and 0.0428 respectively, hence, proving the accuracy of the automated method over the manual method. It was found that whilst the mean %error for our automated method for 5mm crater radius was still improved upon over the manual method it was not significant with a p-value of 0.3087. One reason for this is because it becomes physically easier to discern and delineating craters manually as the crater radii increases. It is conventional to take the manual method as the standard benchmark. However, for crater sizes < 5mm this is not the case and the automated method could serve to replace the manual delineation method as the benchmark. For this reason the automated method was used as the benchmark for real type-IV crater lesions. Furthermore, particularly in respect to the time taken, a knee often would require an order of 30 minutes (for N=3 repeats), for the scans to be processed manually and the crater to be delineated manually, compared to the near instantaneous result attained from the automatic method.

The final section of the paper was concerned with the automatic detection and quantification of real type-IV crater lesions which were independently identified and delineated by an expert. The automated method presented was firstly used to detect knees with pathology from a randomized series of 25 knees (4 with pathology and 21 healthy) and quantify the volumes of the real arthritic craters detected. We demonstrated how the automated method correctly detected 100% of the 25 knees determining whether they had pathology or not. Additionally, the automated method identified the locations of the type-IV craters to be in the same regions identified by an independent operator (blinded to the pathology of the scans) to 100% (Kappa =1). Furthermore, our method, determined how many slices existed in each type-IV crater lesions to 100% accuracy also resulting in a p-value <0.001 when compared to the independent operator. Finally, we determined the volume of the five real type-IV crater lesions using the manual and automated methods. Using our automated method as benchmark we found that the manual method underestimated the crater volume by 1.7% on mean which is consistent with the underestimation observed in the manual delineation of synthetic holes in comparison to our automatic method. Thus, our automated method has the potential to be used as a benchmark for craters ≤ 5 mm radii.

One limitation, with quantifying crater volumes in real human knees is that it is not possible to obtain the true volumes of the craters with a physical experimental measure. In addition, if manual delineation becomes inaccurate for small hole diameters (as we demonstrated in this article) making it increasingly difficult to gauge volumes with benchmark measures such as manual delineation. In this paper, we addressed this issue by performing extensive simulations

with synthetic holes to validate the model. Another limitation is that at this time, the automated was only developed to be applicable to type-IV crater lesions in the femoral cartilage.

5. DISCUSSION AND FUTURE WORK

Up to now no automated image processing strategies have been developed to detect type-IV crater lesions from MR images of the human knee. The only comparative methods that currently exist to identify type-IV crater lesions are typically manual identification from MR images of the knee by either an orthopedic surgeon, experienced in musculoskeletal imaging, or a radiologist [19] to diagnose cartilage lesions typically classified by an Outerbridge grading system [2, 14-17]. The impact of this article, is that demonstrates, for the first time, how the type-IV lesion crater can be detected and quantified automatically with a heuristic geometrical image processing approach. In addition, our developed method would allow for the grading of the lesion size of type-IV craters to be determined which is important in order to make a decision about the treatment [30].

Future directions, would be to extend the image processing techniques developed in this paper in order to identify other OA lesion types, described in Bauer et al 1988 [2].

6. ACKNOWLEDGEMENTS

We would like to acknowledge the financial support by Higher Education Commission (HEC) of Pakistan and University of Auckland PRESS fund.

7. REFERENCES

[1] R. Reid, F. Roberts, R. Callander, and I. Ramsden, Pathology illustrated: Elsevier/Churchill Livingstone, 2005.

[2] M. Bauer and R. Jackson, "Chondral lesions of the femoral condyles: a system of arthroscopic classification," Arthroscopy: The Journal of Arthroscopic & Related Surgery, vol. 4, pp. 97-102, 1988.

[3] K. E. DeHaven and H. Collins, "Diagnosis of internal derangements of the knee. The role of arthroscopy," The Journal of Bone & Joint Surgery, vol. 57, pp. 802-810, 1975.

[4] S. Fischer, J. Fox, W. Del Pizzo, M. Friedman, S. Snyder, and R. Ferkel, "Accuracy of diagnoses from magnetic resonance imaging of the knee. A multi-center analysis of one thousand and fourteen patients," J Bone Joint Surg Am, vol. 73, pp. 2-10, 1991.

[5] J. L. Halbrecht and D. W. Jackson, "Office arthroscopy: a diagnostic alternative," Arthroscopy: The Journal of Arthroscopic & Related Surgery, vol. 8, pp. 320-326, 1992.

[6] O. H. Sherman, J. M. Fox, S. J. Snyder, W. Del Pizzo, M. Friedman, R. Ferkel, et al., "Arthroscopy--" no-problem surgery". An analysis of complications in two thousand six hundred and forty cases," J Bone Joint Surg Am, vol. 68, pp. 256-265, 1986.

[7] N. C. Small, "Complications in arthroscopy: the knee and other joints: committee on complications of the Arthroscopy Association of North America," Arthroscopy: The Journal of Arthroscopic & Related Surgery, vol. 2, pp. 253-258, 1986.

[8] A. A. Kshirsagar, P. J. Watson, J. A. Tyler, and L. D. Hall, "Measurement of localized cartilage volume and thickness of human knee joints by computer analysis of three-dimensional magnetic resonance images," Investigative radiology, vol. 33, pp. 289-299, 1998.

[9] C. G. Peterfy, S. Majumdar, P. Lang, C. Van Dijke, K. Sack, and H. K. Genant, "MR imaging of the arthritic knee: improved discrimination of cartilage, synovium, and effusion with pulsed

saturation transfer and fat-suppressed T1-weighted sequences," Radiology, vol. 191, pp. 413-419, 1994.

[10] M. A. Piplani, D. G. Disler, T. R. McCauley, T. J. Holmes, and J. P. Cousins, "Articular cartilage volume in the knee: semiautomated determination from three-dimensional reformations of MR images," Radiology, vol. 198, pp. 855-859, 1996.

[11] F. Eckstein, H. Sittek, A. Gavazzeni, E. Schulte, S. Milz, B. Kiefer, et al., "Magnetic resonance chondro-crassometry (MR CCM): A method for accurate determination of articular cartilace thickness?," Magnetic Resonance in Medicine, vol. 35, pp. 89-96, 2005.

[12] F. Eckstein, A. Gavazzeni, H. Sittek, M. Haubner, A. Lösch, S. Milz, et al., "Determination of knee joint cartilage thickness using three-dimensional magnetic resonance chondro-crassometry (3D MR-CCM)," Magnetic Resonance in Medicine, vol. 36, pp. 256-265, 2005.

[13] F. Eckstein, C. Adam, H. Sittek, C. Becker, S. Milz, E. Schulte, et al., "Non-invasive determination of cartilage thickness throughout joint surfaces using magnetic resonance imaging," Journal of biomechanics, vol. 30, pp. 285-289, 1997.

[14] R. Ficat, J. Philippe, and D. Hungerford, "Chondromalacia patellae: a system of classification," Clinical orthopaedics and related research, vol. 144, pp. 55-62, 1979.

[15] F. R. Noyes and C. L. Stabler, "A system for grading articular cartilage lesions at arthroscopy," The American journal of sports medicine, vol. 17, pp. 505-513, 1989.

[16] L. Von Engelhardt, A. Schmitz, B. Burian, P. Pennekamp, H. Schild, C. Kraft, et al., "[3-Tesla MRI vs. arthroscopy for diagnostics of degenerative knee cartilage diseases: preliminary clinical results]," Der Orthopade, vol. 37, pp. 914, 916-22, 2008.

[17] J.-S. Suh, S. Lee, E.-K. Jeong, and D.-J. Kim, "Magnetic resonance imaging of articular cartilage," European Radiology, vol. 11, pp. 2015-2025, 2001.

[18] W. W. Curl, J. Krome, E. S. Gordon, J. Rushing, B. P. Smith, and G. G. Poehling, "Cartilage injuries: a review of 31,516 knee arthroscopies," Arthroscopy: The Journal of Arthroscopic & Related Surgery, vol. 13, pp. 456-460, 1997.

[19] S. Kohl, S. Meier, S. S. Ahmad, H. Bonel, A. K. Exadaktylos, A. Krismer, et al., "Accuracy of cartilage-specific 3-Tesla 3D-DESS magnetic resonance imaging in the diagnosis of chondral lesions: comparison with knee arthroscopy," Journal of orthopaedic surgery and research, vol. 10, p. 1, 2015.

[20] A. Årøen, S. Løken, S. Heir, E. Alvik, A. Ekeland, O. G. Granlund, et al., "Articular cartilage lesions in 993 consecutive knee arthroscopies," The American journal of sports medicine, vol. 32, pp. 211-215, 2004.

[21] G. A. Murrell, S. Maddali, L. Horovitz, S. P. Oakley, and R. F. Warren, "The effects of time course after anterior cruciate ligament injury in correlation with meniscal and cartilage loss," The American Journal of Sports Medicine, vol. 29, pp. 9-14, 2001.

[22] R. N. Tandogan, Ö. Taşer, A. Kayaalp, E. Taşkıran, H. Pınar, B. Alparslan, et al., "Analysis of meniscal and chondral lesions accompanying anterior cruciate ligament tears: relationship with age, time from injury, and level of sport," Knee Surgery, Sports Traumatology, Arthroscopy, vol. 12, pp. 262-270, 2004.

[23] J. W. Alford and B. J. Cole, "Cartilage restoration, part 1 basic science, historical perspective, patient evaluation, and treatment options," The American journal of sports medicine, vol. 33, pp. 295-306, 2005.

[24] H. Shim, S. Chang, C. Tao, J.-H. Wang, C. K. Kwoh, and K. T. Bae, "Knee Cartilage: Efficient and Reproducible Segmentation on High-Spatial-Resolution MR Images with the Semiautomated Graph-Cut Algorithm Method," Radiology, vol. 251, pp. 548-556, 2009.

[25] J. H. McDonald, Handbook of biological statistics vol. 2: Sparky House Publishing Baltimore, MD, 2009.

[26] Z. Javaid, M. G. Boocock, P. J. McNair, and C. P. Unsworth, "Contour interpolated radial basis functions with spline boundary correction for fast 3D reconstruction of the human articular cartilage from MR images," Medical Physics, vol. 43, pp. 1187-1199, 2016.

[27] C. Harris and M. Stephens, "A combined corner and edge detector," in Alvey vision conference, 1988, p. 50.

[28] J. Cheong, D. Suter, and F. Cicuttini, "A semi-automatic system for measuring tibial cartilage volume," in TENCON 2005 2005 IEEE Region 10, 2005, pp. 1-6.

[29] B. Caverlieri, "Geometria Indivisibilibus Continuorum: Bononi: Typis Clemetis Feronij, 1635," Reprinted as Geometria degli Indivisibili. Torino: Unione Tipografico-Editorice Torinese, 1966.

[30] T. O. Smith, B. T. Drew, A. P. Toms, S. T. Donell, and C. B. Hing, "Accuracy of magnetic resonance imaging, magnetic resonance arthrography and computed tomography for the detection of chondral lesions of the knee," Knee Surgery, Sports Traumatology, Arthroscopy, vol. 20, pp. 2367-2379, 2012.